Modeling of spacecraft potential measurements on Rosetta

Anders I. Eriksson* and Christian Hånberg†
Swedish Institute of Space Physics, Uppsala

Alexander Sjögren‡
Embry-Riddle Aeronautical University, Daytona Beach, Florida
(Dated: October 4, 2010)

Based on simulation results, we construct a model for the influence of the spacecraft-plasma interaction on measurements of the potential of the Rosetta spacecraft in the solar wind. Rosetta is now en route to comet 67P/Churyomov-Gerasimenko, to follow the comet in its orbit in toward perihelion and investigate the cometary nucleus and its environment. In the tenuous plasmas encountered in the unperturbed solar wind and near the comet during its low-activity phase outside approximately 2.5 AU heliocentric distance, the spacecraft potential is a good proxy for the plasma density. However, the influence of the photoelectron cloud and the solar wind wake complicates the spacecraft potential measurement by the Langmuir probe instrument, so a model of these effects is necessary for correct data interpretation. We describe the model and its parametrization in terms of plasma and photoemission parameters. Good fits are obtained, opening for reduction of errors from these sources to below the 0.1 V level.

I. INTRODUCTION

Among the instruments carried on the Rosetta space probe, destined to follow comet 67/P Churyomov-Gerasimenko in its orbit toward perihelion for at least a year and even to put a small lander on the comet surface [1], is a Langmuir probe instrument, LAP, for studies of the ionized component of the cometary environment [2, 3] as a part of the Rosetta Plasma Consortium (RPC) [4]. The LAP senors are two spherical probes (diameter 5 cm) mounted on short sticks (17.2 cm) at the ends of two solid booms, one of length 2.24 m and the other 1.62 m (Figure 1). In the fully developed coma close to the comet, the Debye length of the plasma will be small compared to the boom length, meaning that the electrostatic field from the spacecraft will have decayed to a small fraction at the location of the probes. However, at the start of comet operations, as well as during the bulk of the about 80 days of operation LAP has seen from the launch in March 2004 up to now (2010), the typical environment seen is the more or less unperturbed solar wind, with Debye length longer than the boom lengths. In this tenuous plasma, the spacecraft potential $V_{\rm s}$ is determined by a balance of spacecraft photoemission and collection of plasma electrons, and therefore is a useful proxy for the plasma density [5–7]. However, because of the long Debye length, the potential measured between probe and spacecraft, $V_{\rm ps}$, will only be a fraction of $V_{\rm s}$ [8].

In addition, $V_{\rm ps}$ will be influenced by some other sources: a contribution $U_{\rm w}$ from the potential due to the space charge in the wake forming behind the spacecraft and its solar panels, and another contribution $U_{\rm f}$ from the cloud of emitted photoelectrons. As shown by particle-in-cell simulations using the SPIS code [9, 10], the potentials from these sources can be significant, and should thus be corrected for. The potentials $U_{\rm w}$ and $U_{\rm f}$ both depend on the pointing of the spacecraft, as the probes move around in the wake and photoelectron cloud when the attitude changes.

For nominal Rosetta operations, the solar panels face the sun at right angles. In addition, we may assume that the solar wind and the sunlight rays are parallel. The pointing is then described by only one angle, which we take to be the solar aspect angle, ϕ, defined in the right panel of Figure 1. Plots of $V_{\rm p}$, the potential in space at the probe position, derived from the particle-in-cell simulations in [9], are shown as functions of ϕ in Figures 2 - 4. To estimate $V_{\rm s}$ from the parameter normally presented as a density proxy [7], the probe-to-spacecraft potential $V_{\rm ps} = V_{\rm p} - V_{\rm s}$, will obviously need an angle-dependent correction, the finding of which is the goal of the present study.

The SPIS simulations of the electrostatic potential in space at the probe positions are reported in an accompanying paper [10] and in more detail in [9]. In the present study, the aim is to find an analytical model enabling us to correct for the pointing effects. We do this in several steps. In Section II, we define a model for the angular dependence of each perturbation source, based on the general characteristics of the simulation results. We then do a least squares

*Electronic address: Anders.Eriksson@irfu.se
†Electronic address: chha0947@student.uu.se
‡Electronic address: sjogrena@my.erau.edu

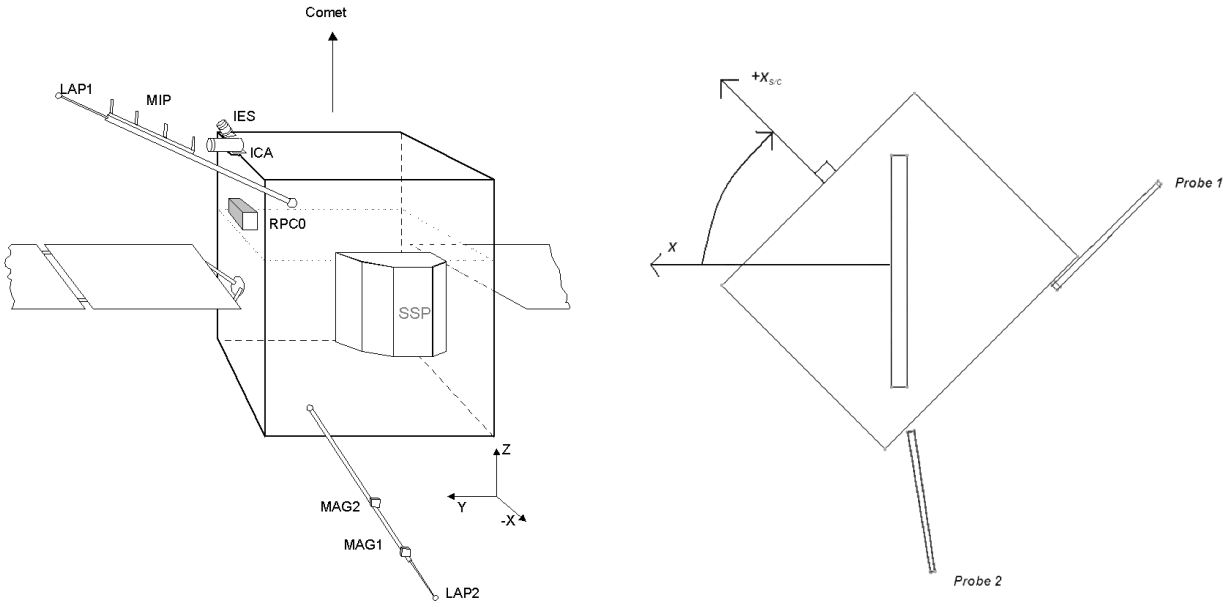

FIG. 1: *Left:* The Rosetta spacecraft body with the lander (marked SSP) and the various units of the Rosetta Plasma Consortium, RPC, including the two Langmuir probes, here identified as LAP1 and LAP2. For further desription, see [4]. *Right:* Rosetta viewed along the solar panels from the $+Y$ direction in spacecraft coordinates. The solar aspect angle, ϕ, describes the pointing of the spacecraft $+X$ axis with respect to the sun.

fit to each simulation results in Section III, thereby establishing an initial idea of how each term depends on the plasma and photoelectron parameters varied between the simulations. For each of these terms, we then investigate the dependence on the plasma and photoelectron parameters in Section IV.

II. PERTURBATION SOURCES

The SPIS simulations [9] will now be used to formulate a model for the angular dependence of the probe voltage. From these simulations, it makes sense to analyze the potential V_p at the probe position in terms of its sources as

$$V_\mathrm{p}(\phi) = U_\mathrm{a} + U_\mathrm{w}(\phi) + U_\mathrm{f}(\phi), \tag{1}$$

where U_a is the potential field from the spacecraft, U_w the potential due to space charge in the wake, and U_f is the potential due to the space charge in the photoelectron cloud. We thus assume these three sources can be separated, which would not hold strictly true in reality but is a good starting point for a model. In addition, we assume that the various terms in this equation will depend on the following parameters:

- Spacecraft potential V_s, which influences the motion of all charges as well as contributes with a strong potential field.
- Electron density n_e and temperature T_e in the solar wind plasma. The solar wind ions have so high energy (keV order) that the basic structure of the wake close to the spacecraft is independent of their detailed properties, so only the electrons need to be considered.
- Photoelectron emission saturation current density j_f0 and typical energy T_f, desribing the photoemission. Values appropriate for emission from the probes can be derived from probe bias sweeps [2], and it can be assumed that for other surfaces, T_f is similar and j_f0 proportional to the value derived from the probes. Typical values for these parameters are in the range of tens of $\mu\mathrm{A/m}^2$ (at Earth orbit) and a few eV, respectively [11], with the photemission current scaling with the solar EUV flux [12] and thus with the inverse square of heliocentric distance.

One may note that we here have listed V_s as an independent parameter. In reality, V_s is set by the requirement that the sum of all currents flowing to space from the spacecraft must be zero, and it is therefore a function of the other

parameters listed above [6]. In the SPIS simulations, it is certainly possible to let V_s be self-consistently determined by this condition, and this is something we plan for later studies. But as the task for the present simulations have been to investigate how to derive V_s from V_ps, not how V_s depends on n_e and T_e, we have chosen the present approach. The spacecraft potential of Rosetta in various situations was simulated in [13].

III. FITTING TO SIMULATIONS

A. Basis functions

The wake and the photoelectron cloud are localized in angle, so a quite obvious ansatz is to model them by Gaussians. We have done so for the $U_\mathrm{w}(\phi)$ as well as for the $U_\mathrm{w}(\phi)$ functions, trying out a variety of parameters for the centres ϕ_w and ϕ_f as well as for the widths ω_w and ω_f of the wake and photoelectron clouds. We found that while a Gaussian worked well for the wake, a slightly sharper shape gave better fits for the photoelectron cloud:

$$U_\mathrm{w} = A_\mathrm{w} \exp\left(- \left[\frac{\phi - \phi_\mathrm{w}}{\omega_\mathrm{w}} \right]^2 \right) \tag{2}$$

$$U_\mathrm{f} = A_\mathrm{f} \exp\left(- \left[\frac{\phi - \phi_\mathrm{f}}{\omega_\mathrm{f}} \right]^{3/2} \right) . \tag{3}$$

Suitable parameter values for the two probes were found to be:

- For probe 1: $\phi_\mathrm{w1} = 65°$, $\phi_\mathrm{f1} = 245°$, $\omega_\mathrm{w1} = 60°$, $\omega_\mathrm{f1} = 90°$
- For probe 2: $\phi_\mathrm{w2} = 325°$, $\phi_\mathrm{f2} = 145°$, $\omega_\mathrm{w2} = 80°$, $\omega_\mathrm{f2} = 90°$

The choice of these basis functions is based on manual trial and error only. It may perhaps be argued that we could use an automatic nonlinear fit routine, minimizing the residual of the fit in e.g. a least-squares sense. In practice, the rather few points and high noise levels in the simulations tend to complicate such fits, and we consider the manual procedure to be more satisfactory. However, finding relevant amplitudes for these basis functions for each simulation run is a task well suited for linear least squares fitting.

B. Fit results

Linear least-squares fitting to the basis functions in Section III A, with a constant representing U_a in each simulation, gives the results displayed in the last six columns of Table I. The fit results are also plotted for each simulation as dotted curves in Figures 2 - 4. For better coverage of parameter space, we have added a few simulations to those in [10], but it should be noted that this space is still very sparsely populated: for example, only two values of V_s have been simulated.

While far from perfect, the fit results illustrated in Figures 2 - 4 are sensible with the exception of some results for the wake signature at the position of probe 2, where some non-physical positive values can be found in Table I. This is due to the comparatively small wake in these instances, combined with the simulation noise and the non-perfect basis functions. In Section IV, we proceed to model the parameter dependence of the fit parameters.

IV. PARAMETRIZATION OF PERTURBATIONS

A. Shielding

We now do the ansatz that shielding effects can be quantified by a single shielding length λ, which in absence of photoemission should be the Debye length. Working with the inverse shielding length $k = 1/\lambda$ is more practical, as k^2 is an additive property at least in the case of linear Debye shielding, with a contribution from each particle population proportional to its density. The shielding due to the surrounding plasma electrons should thus be quantified by

$$k_\mathrm{e}^2 = \frac{ne^2}{\epsilon_0 K T_\mathrm{e}}. \tag{4}$$

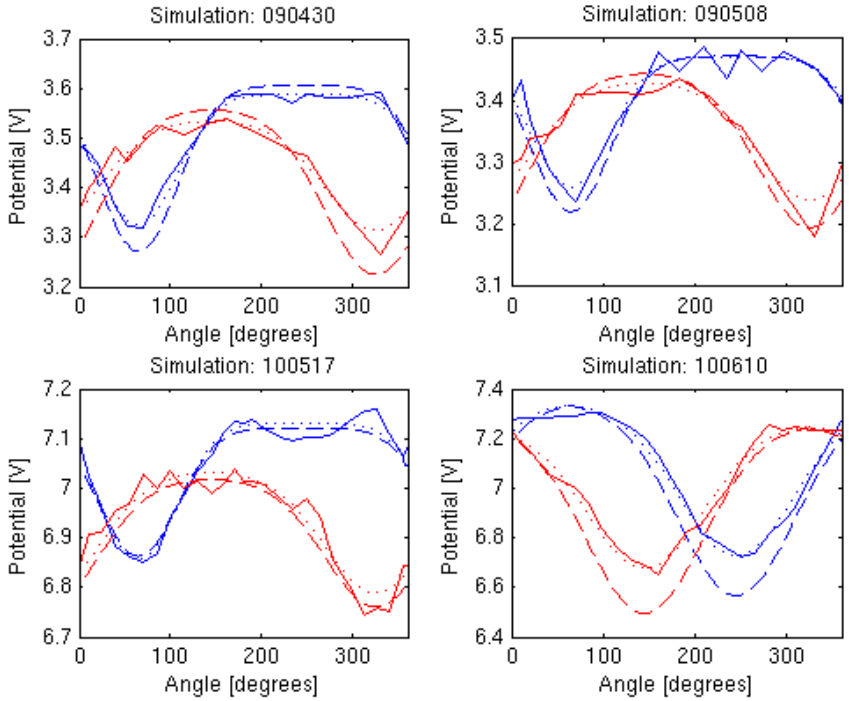

FIG. 2: The potential at the positions of the Rosetta Langmuir probes P1 (blue) and P2 (red) at various solar aspect angles for the first four simulations in Table I. Solid: SPIS simulations. Dotted: Free least squares fits to the simulations. Dashed: Model results. Simulation parameters can be found in Table I.

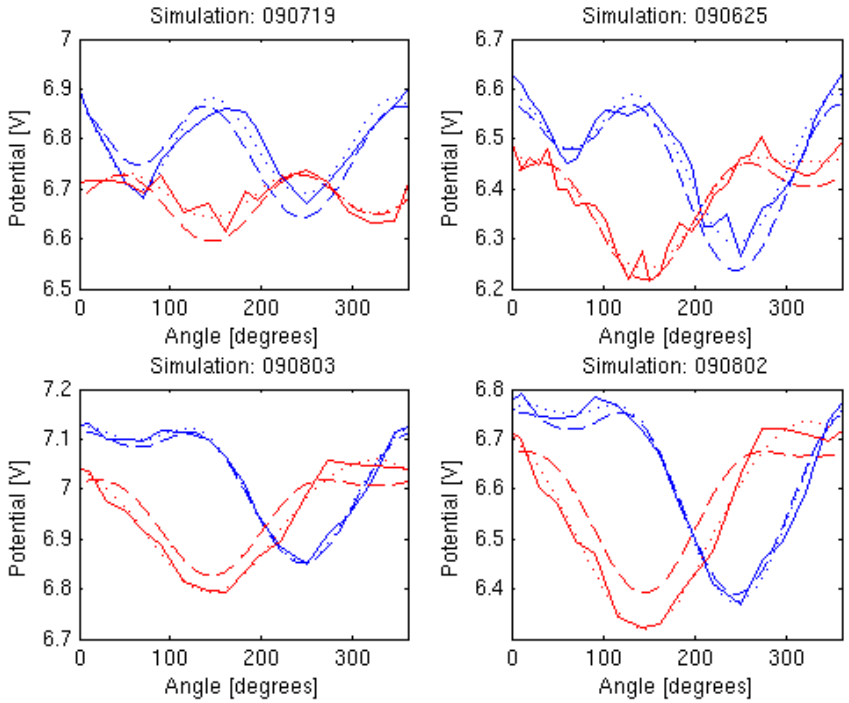

FIG. 3: The potential at the positions of the Rosetta Langmuir probes P1 (blue) and P2 (red) at various solar aspect angles for the second group of four simulations in Table I. Solid: SPIS simulations. Dotted: Free least squares fits to the simulations. Dashed: Model results. Simulation parameters can be found in Table I.

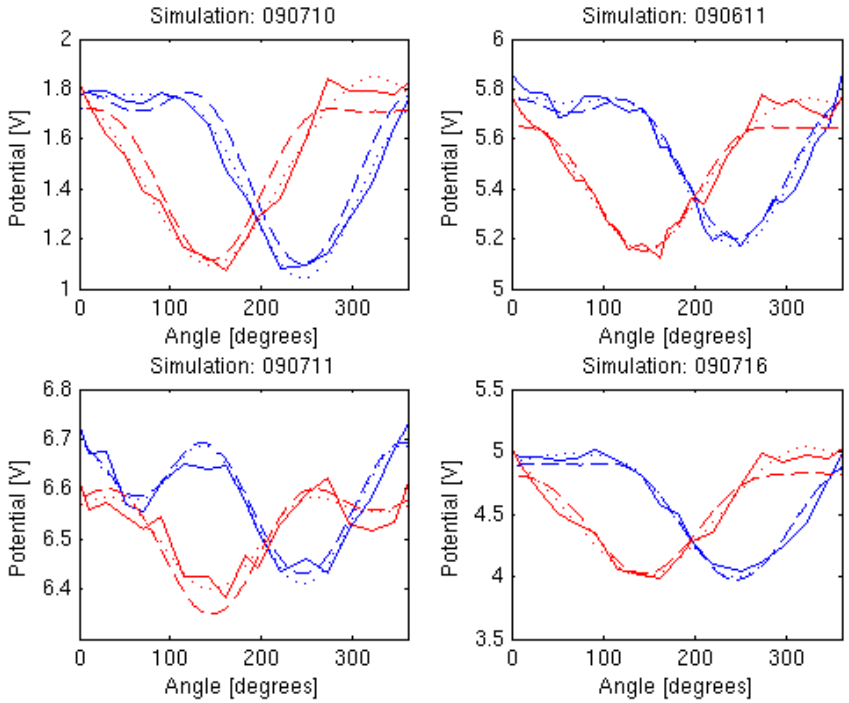

FIG. 4: The potential at the positions of the Rosetta Langmuir probes P1 (blue) and P2 (red) at various solar aspect angles for the last four simulations in Table I. Solid: SPIS simulations. Dotted: Free least squares fits to the simulations. Dashed: Model results. Simulation parameters can be found in Table I.

The ions are here assumed not to contribute to the shielding. This is reasonable for the solar wind, were typical ion energies are around a keV due to the flow, while the electrons, flowing subsonically, have typical energies of a few or at most a few tens of eV.

We assume the photoelectrons are Boltzmann distributed with a characteristic energy KT_f of a few eV [11], so that their typical speed is $v_\mathrm{f} = \sqrt{KT_\mathrm{f}/m_\mathrm{e}}$, neglecting any effects of a high-energy tail [6]. A characteristic photoelectron density can then be calculated from the photoemission saturation current density j_f0 as $n_\mathrm{f} = j_\mathrm{f0}/(ev_\mathrm{f})$. For the inverse

1	2	3	4	5	6	7	8	9	10	11	12	13
Simulation	T_e [eV]	T_i [eV]	T_f [eV]	n [cm^{-3}]	V_s [V]	j_f0 [μA/m^2]	U_{a1} [V]	A_w1 [V]	A_f1 [V]	U_{a2} [V]	A_w2 [V]	A_f2 [V]
090430	12	5	0	5	5	-	3.5880	-0.2637	-	3.5365	-0.2220	-
090508	6	5	0	5	5	-	3.4714	-0.2101	-	3.4299	-0.1897	-
100517	12	5	0	5	10	-	7.1322	-0.2765	-	7.0329	-0.2444	-
100610	-	-	2	0	10	30	7.3485	-	-0.6193	7.2573	-	-0.5800
090719	12	5	2	5	10	3.33	7.0426	-0.3378	-0.3524	6.8804	-0.2217	-0.2355
090625	12	5	2	5	10	7.5	6.7669	-0.2742	-0.4744	6.5971	-0.1350	-0.3562
090803	12	5	2	0.56	10	3.33	7.2307	-0.1248	-0.3735	7.0315	0.0325	-0.2388
090802	12	5	2	1.25	10	7.5	6.9030	-0.1380	-0.5292	6.6753	0.0681	-0.3562
090710	12	5	2	5	5	30	1.9310	-0.1311	-0.8879	1.6891	0.1723	-0.5965
090611	12	5	2	5	10	30	5.9640	-0.2006	-0.7957	5.7539	0.0186	-0.5961
090711	12	5	1	5	10	30	6.8566	-0.2686	-0.4459	6.7478	-0.1869	-0.3467
090716	12	5	4	5	10	30	5.1559	-0.1497	-1.1637	4.7668	0.2872	-0.7644

TABLE I: Simulations and fits. Columns 1 is simulation reference number, columns 2 - 7 plasma and photoelectron parameters used in the simulations, columns 8 - 10 and 11 - 13 results of least squares fitting to the basis functions in Section III A for probe 1 and 2, respectively. The simulations are presented in an accompanying paper [10] and, in more detail, in [9].

shielding length due to photoelectrons, we therefore do the ansatz

$$k_{\rm f}^2 = \frac{n_{\rm f} e^2}{\epsilon_0 K T_{\rm f}} = \frac{j_{\rm f0}\, m_{\rm e}^{1/2} e}{\epsilon_0 (K T_{\rm f})^{3/2}}\,. \tag{5}$$

The total shielding inverse length then can be put to

$$k^2 = k_{\rm e}^2 + \beta k_{\rm f}^2, \tag{6}$$

where an empirical dimensionless constant β, presumably of order unity, is introduced to account for the approximate nature of the reasoning above.

B. Photoelectron cloud

The amplitude $A_{\rm f}$ of the potential due to the photoelectron cloud $U_{\rm f}$ can be expected to increase with increasing photoemission saturation current $j_{\rm f0}$, as this should increase the number of photoelectrons in space. In particular, $A_{\rm f}$ should go to zero with $j_{\rm f0}$, but the dependence may well be weaker than linear, due to space charge effects in the photoelectron cloud. On the other hand, we expect this potential to vary oppositely to the spacecraft potential, because higher spacecraft potential means that many photoelectrons are quickly returned to the spacecraft and reabsorbed. Finally, we may expect a shielding effect. Based on these arguments, a reasonable ansatz is

$$A_{\rm f} = F \frac{j_{\rm f0}^{\gamma}}{(1 + \frac{eV_{\rm s}}{KT_{\rm f}})^{\epsilon}} \exp(-kd)\,. \tag{7}$$

Testing of a series of values gave good fits to the least-squares fitted parameters for both probes with $\gamma = 0.5$ and $\epsilon = 0.4$. For the β parameter in Equation (6), values of 0.25 and 0.5 were found to be suitable for probes 1 and 2, respectively. The $d_{\rm f}$ values and the proportionality constant F also were found to differ for the two probes, with $d_1 = 0.08$ m, $d_2 = 0.10$ m, $F_1 = 0.5$ and $F_2 = 0.4$, where the latter are not dimensionless but in units of $\mathrm{V}\cdot(\mu\mathrm{A/m^2})^{-1/2}$. That parameters vary between the two probes is not strange, as neither the boom lengths or their directions from the spacecraft are similar (Figure 1)

This parametrization, together with the wake model to be described in Section IV C below, are illustrated by dashed curves in Figures 2 - 4. The photoelectron clouds are the potential minima seen around 245 degrees for probe 1 and 145 degrees for probe 2. While the model clearly is far from perfect, it stays well within 100 mV of the simulated values, and in most cases within 50 mV.

C. Wake

The potential in an infinite slab of thickness l, small compared to the Debye length $\lambda_{\rm D}$, from which the ions but not the electrons are removed, scales as $(\lambda_{\rm D}/l)^2 K T_{\rm e}/e$, where the temperature dependence cancels so that we just get a scaling with n. With this in mind, and considering shielding effects, we used an ansatz

$$A_{\rm w} = W n^{\mu} \exp(-k_{\rm e} b) \tag{8}$$

for the amplitude of the wake potential. Initially, we used the combined plasma and photoelectron shielding parameter k in the exponential, but better fits were obtained when using the plasma electron shielding inverse length $k_{\rm e}$ only. We found that the same expression and values worked quite well for both probes, with $\mu = 1/3$, $b = 0.9$ m and $W = 0.3$ V·cm. It can be seen by comparing the model results (dashed) to the simulation results (solid) in Figures 2 - 4 that the wake (which is seen around 65 degrees for probe 1 and 325 degrees for probe 2) is reasonably but not perfectly modeled. In the first three simulations, in which there are no photoelectrons, the wake signature is very well modelled, and in general the model works very well for probe 1 in all simulations. For probe 2, the wake contribution seems underestimated at least in the last three simulations. However, as the wake generally is rather small, the modeled wake amplitude always stays within 100 mV of the simulated wake signature.

V. CONCLUSION

In this study, we have presented a parametrization of the angular dependence seen in PIC simulations of the potential at the positions of the two Langmuir probes on Rosetta in the solar wind. We constructed a model based on

simple physical arguments and tuned it to obtain good fits with simulation data. The resulting expressions make it possible to estimate the influence of wake and photoelectrons on the probe voltage data from this instrument, so that confidence limits on such data can be established. This is particularly important as the first signatures of activity on the target comet will be picked up in an environment dominated by the solar wind. and a model like this is necessary so that data with confidence limits can be quickly supplied to the scientific community when arriving at the comet in 2014.

While the simple models used very well reproduce the simulations, there remains several issues. First, it would be useful to also model the parametric dependencies of the constant term U_a in Equation (1). Second, there is clearly room for improvement of our model. Comparing simulated, fitted, and modeled data in Figures 2 - 4, it seems that the quasi-Gaussian basis functions we have used could be replaced by functions more triangular in shape, at least for the photoelectron signature. In addition, the wake in particular could have its parametric dependencies better modeled. Finally, the most important task is to compare to real data obtained in space. Such data have been gathered during the Rosetta cruise phase, and this study provides a new tool analyzing and understanding this data set.

Acknowledgments

AS acknowledges support from the US Air Force Research Laboratory for presenting this work at SCTC-11, and thanks David Rodgers and Simon Clucas at ESA/ESTEC for hospitality and help in setting up SPIS simulations.

[1] K. Glassmeier, H. Boehnhardt, D. Koschny, E. Kührt, and I. Richter, "The Rosetta Mission: Flying Towards the Origin of the Solar System," *Space Sci. Rev.*, vol. 128, pp. 1–21, Feb. 2007.

[2] A. I. Eriksson, R. Boström, R. Gill, L. Åhlén, S.-E. Jansson, J.-E. Wahlund, M. André, A. Mälkki, J. A. Holtet, B. Lybekk, A. Pedersen, L. G. Blomberg, and the LAP team, "RPC-LAP: The Rosetta Langmuir probe instrument," *Space Sci. Rev.*, vol. 128, pp. 729–744, doi:10.1007/s11214–006–9003–3, 2007.

[3] A. I. Eriksson, R. Gill, J.-E. Wahlund, M. André, A. Mälkki, B. Lybekk, A. Pedersen, J. A. Holtet, L. G. Blomberg, and N. J. T. Edberg, "RPC-LAP: The Langmuir probe instrument of the Rosetta plasma consortium," in *Rosetta - ESA's Mission to the Origin of the Solar System* (R. Schulz, C. Alexander, H. Boehnhardt, and K.-H. Glassmeier, eds.), Springer, 2008.

[4] C. Carr, E. Cupido, C. G. Y. Lee, A. Balogh, T. Beek, J. L. Burch, C. N. Dunford, A. I. Eriksson, R. Gill, K. H. Glassmeier, R. Goldstein, D. Lagoutte, R. Lundin, K. Lundin, B. Lybekk, J. L. Michau, G. Musmann, H. Nilsson, C. Pollock, I. Richter, and J. G. Trotignon, "RPC: The Rosetta plasma consortium," *Space Sci. Rev.*, vol. 128, pp. 629–647, doi:10.1007/s11214–006–9136–4, 2007.

[5] A. Pedersen, C. Nairn, R. Grard, and K. Schwingenschuh, "Derivation of electron densities from differential potential measurements upstream and downstream of the bow shock and in the magnetosphere of Mars," *J. Geophys. Res.*, vol. 96, pp. 11243–+, July 1991.

[6] A. Pedersen, "Solar wind and magnetosphere plasma diagnostics by spacecraft electrostatic potential measurements," *Ann. Geophysicae*, vol. 13, pp. 118–129, 1995.

[7] A. Pedersen, B. Lybekk, M. André, A. Eriksson, P.-A. Lindqvist, F. Mozer, P. M. E. Décréau, A. Masson, H. Laakso, H.Rème, J.-A. Sauvaud, A. Fazakerley, K. Svenes, G. Paschmann, K. Torkar, and E. Whipple, "Electron density estimations derived from spacecraft potential measurements on Cluster in tenuous plasma regions," *J. Geophys. Res.*, vol. 113, pp. A07S33, doi:10.1029/2007JA012636, 2008.

[8] C. Cully, R. E. Ergun, and A. I. Eriksson, "Electrostatic structure around spacecraft in tenuous plasmas," *J. Geophys. Res.*, vol. 112, pp. A09211, doi:10.1029/2007JA012269, 2007.

[9] A. Sjögren, *Modelling of Rosetta Langmuir probe measurements*. No. UPTEC F09 063, Swedish Institute of Space Physics, Uppsala, and Department of Physics and Astronomy, Uppsala University, 2009.

[10] A. Sjögren, A. I. Eriksson, and C. M. Cully, "Simulations of spacecraft sheath impact on Langmuir probe measurements," in *Proceedings of the 11th Spacecraft Charging Technology Conference*, this volume, 2010.

[11] R. J. L. Grard, "Properties of satellite photoelectron sheath derived from photoemission laboratory studies," *J. Geophys. Res.*, vol. 78, pp. 2885–2906, 1973.

[12] L. H. Brace, W. R. Hoegy, and R. F. Theis, "Solar EUV measurements at Venus based on photoelectron emission from the Pioneer Venus Langmuir probe," *J. Geophys. Res.*, vol. 93, pp. 7282–7296, 1988.

[13] J.-F. Roussel and J.-J. Berthelier, "A study of electrical charging of the Rosetta orbiter: 1. numerical model," *J. Geophys. Res.*, vol. 109, pp. A01104, doi:10.1029/2003JA009836, 2004.